Electrical Power and Energy Systems 83 (2016) 229–240

Contents lists available at ScienceDirect

Electrical Power and Energy Systems

journal homepage: www.elsevier.com/locate/ijepes

Power quality improvement in distribution network using DSTATCOM with battery energy storage system

Om Prakash Mahela *, Abdul Gafoor Shaik

Department of Electrical Engineering, Indian Institute of Technology Jodhpur, 342011, India

ARTICLE INFO

Article history:
Received 14 May 2015
Received in revised form 22 March 2016
Accepted 4 April 2016

Keywords:
Battery energy storage system
Radial distribution feeder
DSTATCOM
Power quality
Synchronous reference frame theory
Wind energy

ABSTRACT

The distribution static compensator (DSTATCOM) provides fast control of active and reactive powers to enable load compensation, harmonics current elimination, voltage flicker mitigation, voltage and frequency regulation. This paper presents power quality improvement technique in the presence of grid disturbances and wind energy penetration using DSTATCOM with battery energy storage system. DSTATCOM control is provided based on synchronous reference frame theory. A modified IEEE 13 bus test feeder with DSTATCOM and wind generator is used for the study. Power quality events during grid disturbances such as feeder tripping and re-closing, voltage sag, swell and load switching have been studied in association with DSTATCOM. The power quality disturbances due to wind generator outage, synchronization and wind speed variations have also been investigated. The study has been carried out using MATLAB/SIMULINK and the simulation results are compared with real time results obtained by the use of real time digital simulator (RTDS) for validating the effectiveness of proposed methodology. The proposed method has been proved to be effective in improvement of power quality with all disturbances stated above.

Introduction

Power quality (PQ) has been a topic of consideration for last twenty years to both utility and end use customers. It has recently acquired intensified interest due to wide use of power electronics, microprocessor based devices, controllers in industrial processes, non linear loads and proliferation of computer network [1]. Further, the grid integration of distributed generation (DG) such as wind, fuel cell, and solar photovoltaic also affects the quality of supplied power [2]. Power quality is any deviation in current, voltage and frequency from their standard values which results in failure or miss operation of customer equipments [3]. PQ is attributed to the various disturbances such as harmonics, voltage flicker, multiple notches, voltage sag, swell, momentary interruption, impulsive and oscillatory transients [4]. The mathematical techniques such as Fourier transform (FT), short time Fourier transform (STFT), S-transform, Hilbert Huang transform, and wavelet transform are used for detection of PQ disturbances. Artificial intelligent (AI) techniques such as support vector machine, neural network, fuzzy expert system, genetic algorithm are used for classification of PQ events. Different PQ detection and classification techniques have been reported in [5]. Both the passive and active filters are used for PQ improvement. A group of controllers known as custom power devices such as unified power quality conditioner (UPQC), dynamic voltage restorer (DVR), and distribution static compensator (DSTATCOM) are used for improving the quality of electrical power [6]. Mahela and Shaik [7], presented the detailed analysis of various power quality improvement techniques.

The distribution static compensator is a voltage source converter (VSC) based device usually supported by short-time energy stored in the dc link capacitor. It can compensate for reactive power, load unbalancing, voltage variations and current harmonics in the distribution network [8]. Performance of the DSTATCOM depends on estimation of active and reactive powers, harmonic currents, and control algorithm used for estimation of reference currents [9]. The control techniques of DSTATCOM like instantaneous $p-q$ theory, synchronous reference frame theory (SRF), modified synchronous reference frame theory (MSRF), instantaneous symmetrical control theory, and average unit power factor theory (AUPF) have been reported in the literature [10]. The battery energy storage system (BESS) connected to the dc bus in parallel with dc link capacitor improves the dynamic performance of the system such as frequency and voltage regulation. The battery

* Corresponding author.
E-mail addresses: opmahela@gmail.com (O.P. Mahela), saadgafoor@iitj.ac.in (A.G. Shaik).

http://dx.doi.org/10.1016/j.ijepes.2016.04.011
0142-0615/

energy storage system provides the additional capacity of DSTATCOM for load balancing, reactive power compensation, harmonic current elimination, and also functions as un-interruptible power supply (UPS) [11]. Detailed analysis of DSTATCOM topologies and control techniques for the improvement of power quality has been reported in [12].

Implementation of the DSTATCOM, addressing power quality improvement, for specific applications such as isolated wind power generation, residential low voltage network, load compensation, isolated asynchronous generator, standalone solar photovoltaic system and water pumping system has been reported in the literature. However, very less number of articles are available for implementation of DSTATCOM at grid level addressing PQ improvement specifically with renewable energy sources. Ghosh and Joshi [13], proposed a DSTATCOM with battery energy storage system for voltage regulation in the mini custom power park. The voltage flicker mitigation of electric arc welder has been achieved using DSTATCOM with BESS and reported in [14]. The improvement of load voltage for a constant speed wind energy system supplying the power to inductive load has been achieved with the help of Fuzzy logic based control of DSTATCOM in [15]. Singh et al. [16], proposed the DSTATCOM for compensation of linear and non-linear loads in both steady state and dynamic conditions. The self-charging control technique of DSTATCOM for mitigation of voltage sag, swell and momentary interruption has been proposed in [17]. The power quality improvement with wind energy system has been presented by the authors in [18].

This paper proposes the implementation of DSTATCOM with battery energy storage system in the three phase balanced distribution network addressing PQ issues. Synchronous reference frame theory based control algorithm is used for the control of DSTATCOM. The power quality improvement during disturbances in the grid due to feeder tripping, feeder re-closing, load switching, voltage sags and swells have been investigated. Power quality events with wind energy operations such as outage of wind generator, grid synchronization of wind generator and wind speed variations have also been investigated. The study has been carried out using MATLAB/SIMULINK and the simulation results are compared with real time results based on the real time digital simulator (RTDS) for validating the effectiveness of proposed system. Based on the studies, it is concluded that the SRF based control of DSTATCOM is easy to implement at grid level for reducing the total harmonic distortion below 5% as per IEEE-519 standard even with wind energy penetration into the grid. Hence, main contribution of present work is the design and implementation of SRF control theory based DSTATCOM with BESS at grid level for PQ improvement. Addressing the PQ improvement during the wind operations such as outage of wind generator, grid synchronization of wind generator and wind speed variations is a new contribution to the earlier studies. The reported literature only focusses on the disturbances due to the design constraints of the converter and wind generator where wind generator operation part is missing which has been addressed in this study.

This paper is divided into five sections. Section "Proposed power quality improvement strategy and test system" describes the proposed PQ improvement strategy, IEEE-13 bus test system, wind generator, DSTATCOM topology utilized for the study and control algorithm used for the control of DSTATCOM. The important mathematical design considerations of the proposed system have also been described in the Section "Proposed power quality improvement strategy and test system". The simulation results and their discussions are presented in Section "Simula tion results and discussion". The real time validation of simulation results utilizing the RTDS is presented in the Section "Real time validation of results". Finally, the conclusions are drawn in the Section "Conclusion".

Proposed power quality improvement strategy and test system

This section details the proposed strategy for mitigation of power quality disturbances in the distribution system caused due to grid disturbances, wind generator operations and wind speed variations. The test system utilized for the study, DSTATCOM topology and design of parameters, control technique used for the control of DSTATCOM and proposed strategy have been detailed in the following subsections.

Test system

This subsection describes the proposed test system and wind generator utilized for the study.

IEEE 13 bus test feeder

The proposed study is carried out using a modified IEEE 13 bus test system. The original system is a 60 Hz, 5 MVA radial distribution feeder with voltage levels of 4.16 kV and 0.48 kV feeding balanced and unbalanced loads [19]. The original test feeder is modified to incorporate the DSTATCOM with battery energy storage system (BESS) and wind generator as shown in Fig. 1. In the proposed study DSTATCOM is connected at bus 632 and wind generator is connected at bus 680 through a transformer (XWG). In Indian power system, the renewable energy (RE) sources are installed at remote locations situated far away from the load centres where land is easily available and connected to the transmission network through local network developed for the RE sources. Therefore, we have selected bus 680 for wind connection and bus 632 near grid integration point for installation of DSTATCOM. The feeder and load characteristics are provided in Tables 1 and 2 respectively. The feeder is connected to the utility grid via a substation transformer. The transformer connected between the nodes 633 and 634 is XFM-1. Transformer characteristics are given in Table 3. The voltage regulator between nodes 650 and 632 is realized by on load tap changer (OLTC) transformer.

All the system feeders are three phase with three phase balanced loads where considered. The aerial feeders use configuration 601 with phase conductor type 556, 500, 26/7 ACSR and

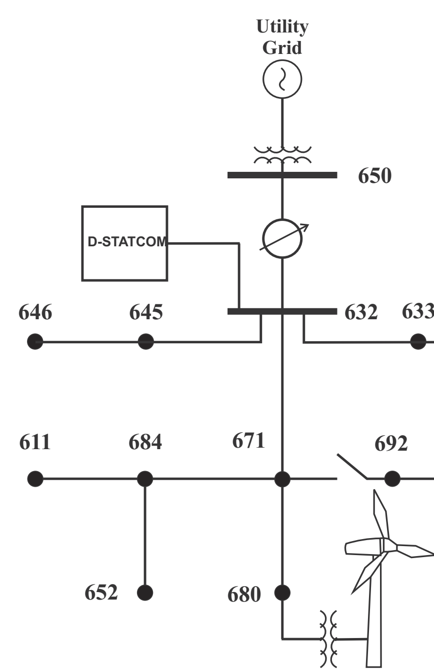

Fig. 1. Modified IEEE 13 bus test system.

Table 1
Feeder data.

Bus A	Bus B	Length (m)	Configuration
632	645	152.4	601
632	633	152.4	601
633	634	0	XFM-1
645	646	91.44	601
650	632	609.6	601
684	652	243.84	606
632	671	609.6	601
671	684	680	601
671	692	0	Switch
684	611	91.44	601
692	675	152.4	606

Table 2
Loading status.

Bus	Load model	Total load		Capacitor kVAr
		kW	kVAr	
632	Y-PQ	100	58	
634	Y-PQ	400	290	
645	Y-PQ	170	125	
646	Y-PQ	230	132	
652	Y-PQ	128	86	
671	Y-PQ	1255	718	
675	Y-PQ	843	462	600
692	Y-PQ	170	151	
611	Y-PQ	170	80	100

Table 3
Transformer data.

Transformer	kVA	kV-high	kV-low	R (%)	X (%)
Substation	5000	115-D	4.16-Gr.Y	1	8
XFM-1	500	4.16-Gr.Y	0.48-Gr.Y	1.1	2
XWG	500	4.16-Gr.Y	0.575-Gr.Y	0.8	1.8

neutral conductor type 4/0, 6/1 with spacing ID 505, while the underground cables use configuration 606 with conductor 250, 000 AA, CN with spacing ID 515. According to the type of conductors and topology of the feeders the series impedance matrices of the test feeders in Ω/km are given by the following relations [20].

$$Z_{601} = \begin{bmatrix} 0.2153+j0.6325 & 0.0969+j0.3117 & 0.0982+j0.2632 \\ 0.0969+j0.3117 & 0.2097+j0.6511 & 0.0954+j0.2392 \\ 0.0982+j0.2632 & 0.0954+j0.2392 & 0.2121+j0.6430 \end{bmatrix} \quad (1)$$

$$Z_{606} = \begin{bmatrix} 0.2153+j0.6325 & 0.0969+j0.3117 & 0.0982+j0.2632 \\ 0.0969+j0.3117 & 0.2097+j0.6511 & 0.0954+j0.2392 \\ 0.0982+j0.2632 & 0.0954+j0.2392 & 0.2121+j0.6430 \end{bmatrix} \quad (2)$$

where Z_{601} and Z_{606} are the series impedance matrices for the feeder configurations 601 and 606 respectively. The positive and zero sequence capacitances for configuration 601 are 1.57199 nF/km and 1.3398 nF/km respectively while for configuration 606 both positive and zero sequence capacitances are equal to 15.96979 μF/km.

Wind generator

The doubly-fed induction generator with capacity 1.5 MW, output voltage of 575 V at frequency of 60 Hz is used as wind generator. The rated wind speed is 11 m/s. Other wind turbine, generator and controller data as reported in [21] are used in the present study. A comprehensive overview of grid interfaced wind technologies has been reported in [22] which provides easy understanding of various technical aspects of grid connected wind energy conversion system.

Proposed DSTATCOM

The three-leg topology of three-phase three-wire DSTATCOM with battery bank proposed for power quality improvement and load compensation in the distribution test feeder is shown in Fig. 2. The point of common coupling (PCC) is selected between the utility grid and the IEEE 13 bus test feeder for connection of proposed DSTATCOM. This DSTATCOM consists of AC inductor, ripple filter, dc link capacitor, battery bank, and three-leg voltage source converter. Insulated gate bipolar transistors (IGBTs) with anti-parallel diodes are used as switches of the voltage source converter (VSC). The combination of six switches in Fig. 2 represents the voltage source converter.

Principle of operation of the proposed DSTATCOM is based on the real and reactive powers that can be exchanged between the PCC and inverter output of the DSTATCOM [23]. The active power (P) and reactive power (Q) exchange between DSTATCOM and PCC are given by the following relations

$$P = \frac{V_{PCC} V_C \sin\alpha}{X} \quad (3)$$

$$Q = \frac{V_{PCC}(V_{PCC} - V_C \cos\alpha)}{X} \quad (4)$$

where α is the angle between the bus and inverter output voltages, V_C is magnitude of inverter output voltage, V_{PCC} is magnitude of PCC voltage, and X is the reactance between the PCC and inverter output terminals. The design of various components of DSTATCOM are detailed in the following subsections.

DC link capacitor

The capacitor connected on dc side of the VSC is known as dc link capacitor (C_{dc}). The design of this capacitor depends on the ability of VSC to regulate voltage during transients [24]. DC link capacitor injects or absorbs active power during transients to maintain the load demand. The value of this capacitor depends upon the minimum and maximum battery voltages and instantaneous energy available to the DSTATCOM during transients [25,26]. The value of dc link capacitor is given by Eq. (5) based on the principle of energy conservation [27].

$$\frac{1}{2} C_{dc} \left[V_{dc}^2 - V_{dc1}^2 \right] = 3VaIt \quad (5)$$

where V_{dc1} is minimum voltage level of dc bus; V is the phase voltage; t is the time by which dc bus voltage is to be recovered, and I is the phase current. Taking, $V_{dc1} = 6970$ V, $V_{dc} = 7000$ V, $V = 2.402$ kV, $I = 486$ A, $t = 350$ μs, and $a = 1.2$, the calculated value of dc link capacitor is approximately 7000 μF. The design value of dc link capacitor used in this study is 10,000 μF.

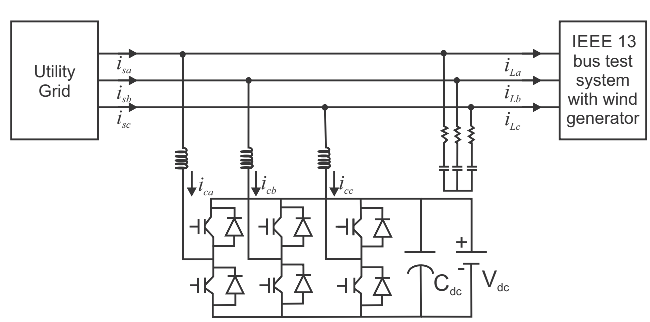

Fig. 2. Proposed DSTATCOM with BESS.

AC inductor

The interfacing inductor (L_f) is connected on ac side of three-leg VSC between VSC and PCC. For successful operation of the DSTATCOM, voltage drop across the interfacing inductor should not be greater than 8% [28]. The design value of L_f is given by the following relation [29].

$$L_f = \frac{\sqrt{3}mV_{dc}}{12af_sI_{cr(p-p)}} \tag{6}$$

where f_s is switching frequency; V_{dc} is dc bus voltage; a is overload factor and $I_{cr(p-p)}$ is peak to peak current ripple. Taking, $I_{cr(p-p)} = 2.5\%$, $V_{dc} = 7000$ V, $f_s = 10$ kHz, $a = 1.2$, and $m = 1$, the L_f is calculated to be 34 mH. A design value of 40 mH is selected in this study.

Ripple filter

A high pass first order filter consisting of series resistor (R_f) and capacitor (C_f) tuned at half the switching frequency is utilized as the ripple filter. It is connected in shunt to the system and used to filter out noise from the voltage at PCC [30]. The time constant of the ripple filter is very small compared to the fundamental time constant (T) and should satisfy the following condition [31]

$$R_fC_f \ll T/10 \tag{7}$$

$R_f = 0.1\ \Omega$ and $C_f = 10\ \mu$F are used as design values in this study.

Battery bank

A battery bank (V_{dc}) is connected in parallel with the dc link capacitor as shown in Fig. 2. For satisfactory operation of the DSTATCOM, dc link voltage should be more than twice the peak value of phase voltage of the ac system [32]. Hence, the dc link voltage opted is given by the following relation [33].

$$V_{dc} = \frac{2\sqrt{2}V_{LL}}{\sqrt{3}m} \tag{8}$$

where m is modulation index and V_{LL} is ac line voltage at PCC. Here, calculated value of V_{dc} is 6793 V for $m = 1$ and $V_{LL} = 4.16$ kV. The battery voltage in this study is kept at 7000 V.

Proposed control of DSTATCOM

The controller for VSC of the DSTATCOM generates reference source currents using SRF theory with carrier based pulse width modulation (PWM) technique [34,35] as shown in Fig. 3. SRF theory based controller involves the sensing of line voltages and load currents. The Clark's transformation is used to convert three-phase instantaneous load currents (I_{La}, I_{Lb}, I_{Lc}) into two-phase currents (I_α, I_β) in stationary frame using the following relation.

$$\begin{bmatrix} I_\alpha \\ I_\beta \end{bmatrix} = \sqrt{\frac{2}{3}}\begin{bmatrix} 1 & -\frac{1}{2} & -\frac{1}{2} \\ 1 & \frac{\sqrt{3}}{2} & -\frac{\sqrt{3}}{2} \end{bmatrix}\begin{bmatrix} I_{La} \\ I_{Lb} \\ I_{Lc} \end{bmatrix} \tag{9}$$

The park's transformation is used to convert currents in stationary frame to synchronously rotating frame known as $d-q$ components (I_d, I_q) as given by the following relation.

$$\begin{bmatrix} I_d \\ I_q \end{bmatrix} = \begin{bmatrix} \cos\theta & \sin\theta \\ -\sin\theta & \cos\theta \end{bmatrix}\begin{bmatrix} I_\alpha \\ I_\beta \end{bmatrix} \tag{10}$$

where θ is transformation angle. The $\cos\theta$ and $\sin\theta$ are obtained from phase voltages using phase locked loop (PLL) technique. The $d-q$ components of current are passed through the low pass filter to extract the dc components (I_{ddc}, I_{qdc}). The active power component of fundamental reference source current (I^*_{ddc}) is generated by limiting the active power component between 85% and 100% of the rated load in the IEEE 13 bus network without considering the wind generation. DSTATCOM supplies real power when load becomes more than rated load (100%) and it absorbs the same when load becomes less than 85% of the rated value. In the presence of wind generation, the power drawn by the test system is less than 85% of rated value which results in the power absorbed by the DSTATCOM.

The phase voltages at PCC are calculated from any two line voltages by the following relation.

$$\begin{bmatrix} V_A \\ V_B \\ V_C \end{bmatrix} = \frac{1}{3}\begin{bmatrix} 2 & 1 \\ -1 & 1 \\ -1 & -2 \end{bmatrix}\begin{bmatrix} V_{AB} \\ V_{BC} \end{bmatrix} \tag{11}$$

The phase voltages are used to calculate the amplitude of instantaneous terminal voltage at PCC using the following relation

$$V_t = \sqrt{\frac{2}{3}\left(V_A^2 + V_B^2 + V_C^2\right)} \tag{12}$$

The voltage error input to the PI controller is given as

$$V_{error} = V_{tref} - V_t \tag{13}$$

where V_{tref} is the reference terminal voltage which is taken as 1 pu in this study.

Reactive power component of fundamental reference source current (I^*_{qdc}) is generated by subtracting reactive power component from output of the PI controller. These active and reactive power components of fundamental reference source currents are used to generate three-phase fundamental reference source currents ($I^*_{sa}, I^*_{sb}, I^*_{sc}$).

The active and reactive power components of fundamental reference source currents are used to generate the three-phase reference source currents using inverse Park's and Clark's transformation as given in Eqs. (14) and (15) respectively.

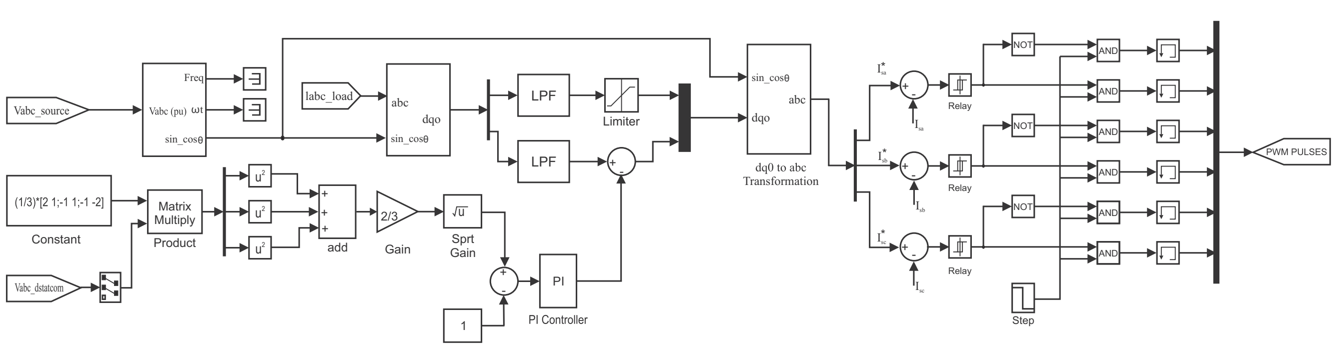

Fig. 3. Proposed SRF based control technique.

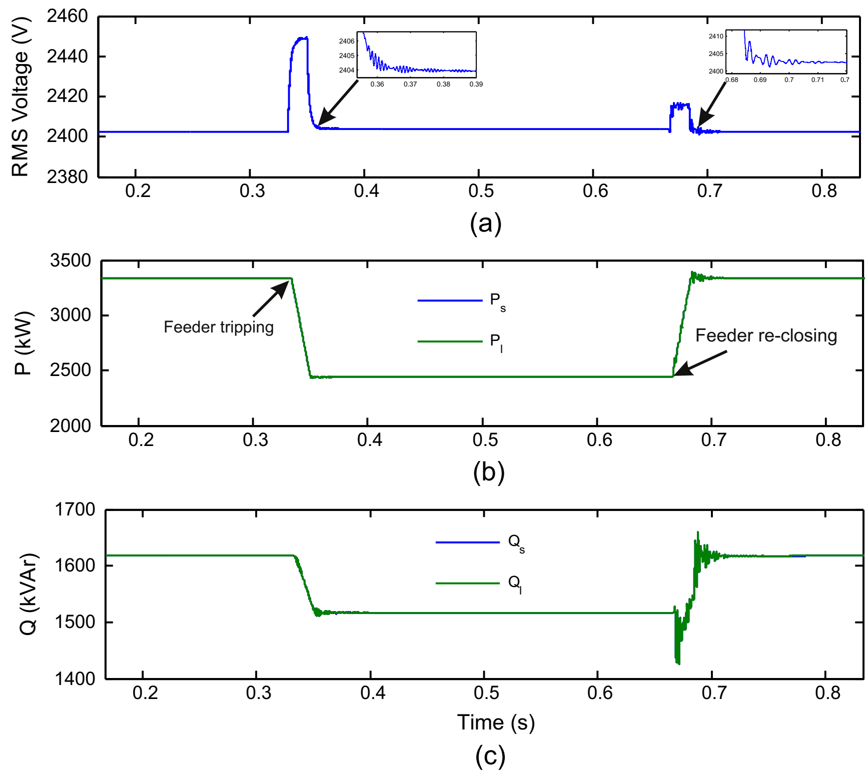

Fig. 4. Feeder tripping and re-closing without DSTATCOM in the network (a) RMS voltage at bus 632, (b) active power flow and (c) reactive power flow.

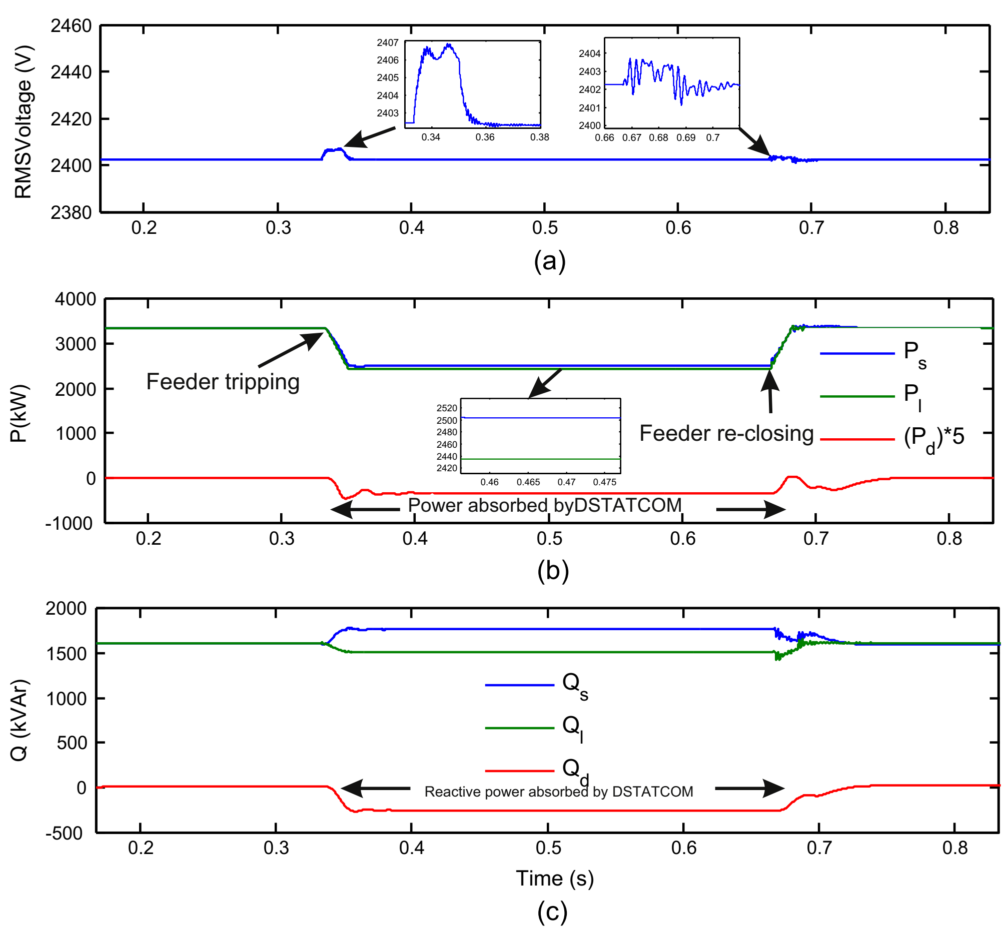

Fig. 5. Feeder tripping and re-closing with DSTATCOM in the network (a) RMS voltage at bus 632, (b) active power flow and (c) reactive power flow.

$$\begin{bmatrix} I^*_{\alpha dc} \\ I^*_{\beta dc} \end{bmatrix} = \begin{bmatrix} \cos\theta & \sin\theta \\ -\sin\theta & \cos\theta \end{bmatrix} \begin{bmatrix} I^*_{ddc} \\ I^*_{qdc} \end{bmatrix} \tag{14}$$

$$\begin{bmatrix} I^*_{sa} \\ I^*_{sb} \\ I^*_{sc} \end{bmatrix} = \sqrt{\frac{2}{3}} \begin{bmatrix} 1 & 0 \\ -\frac{1}{2} & \frac{\sqrt{3}}{2} \\ -\frac{1}{2} & -\frac{\sqrt{3}}{2} \end{bmatrix} \begin{bmatrix} I^*_{\alpha dc} \\ I^*_{\beta dc} \end{bmatrix} \tag{15}$$

The reference source currents obtained in Eq. (15) are compared with the source currents (I_{sa}, I_{sb}, I_{sc}) captured at PCC and current error signal is generated. This error signal is used to generate the pulse width modulation (PWM) signals by hysteresis PWM controller which are utilized as gate signal for the IGBT of voltage source converter.

Proposed PQ improvement strategy

The DSTATCOM with BESS is connected on the bus 632 of the IEEE-13 bus test feeder. A wind generator and a load comprising of 500 kW and 500 kVAr are connected to the bus 680 through circuit breaker. The voltage at bus 632 and current flowing between the utility grid and test feeder are continuously tracked with the help of SRF theory based controller. An error signal is generated based on the reference source current and captured source current. This error signal is utilized to generate the PWM signals for gating the IGBTs of the VSC which controls the active and reactive power flow between the PCC and DSTATCOM. The error signal will be generated depending on the variations in the standard values of voltage and current. Hence, the SRF theory based control of DSTATCOM with BESS can be effectively utilized for PQ improvement at grid level under various case studies.

Simulation results and discussion

This section presents the MATLAB/Simulink based simulation results. The power injected by the utility grid and consumed by the load are considered as positive. The DSTATCOM is considered as source of active and reactive powers if power flows out of the DSTATCOM whereas it acts as load if power is absorbed. The real power supplied by the DSTATCOM (P_d) can be expressed in terms of utility grid power (P_s) and load power (P_l) by the following relation

$$P_d = P_l - P_s \tag{16}$$

The P_d is considered positive for power flows from DSTATCOM to the load and vice versa. Similarly, the reactive power supplied by the DSTATCOM (Q_d) can be expressed in terms of reactive powers of utility grid (Q_s) and load (Q_l) by the relation

$$Q_d = Q_l - Q_s \tag{17}$$

For reactive power flow from DSTATCOM to the grid, Q_d is positive and vice versa.

The DSTATCOM exchanges no active and reactive powers in the absence of wind generation and with the rated load connected to the network. Power exchange is observed in the event of load changes and wind generation. Voltage for the proposed study has been captured at bus 632.

Grid disturbances

Investigations have been made in the events such as feeder tripping and re-closing, voltage sag, swell, and load switching with and without DSTATCOM. The active power, reactive power and harmonic compensations have been analyzed in these investigations.

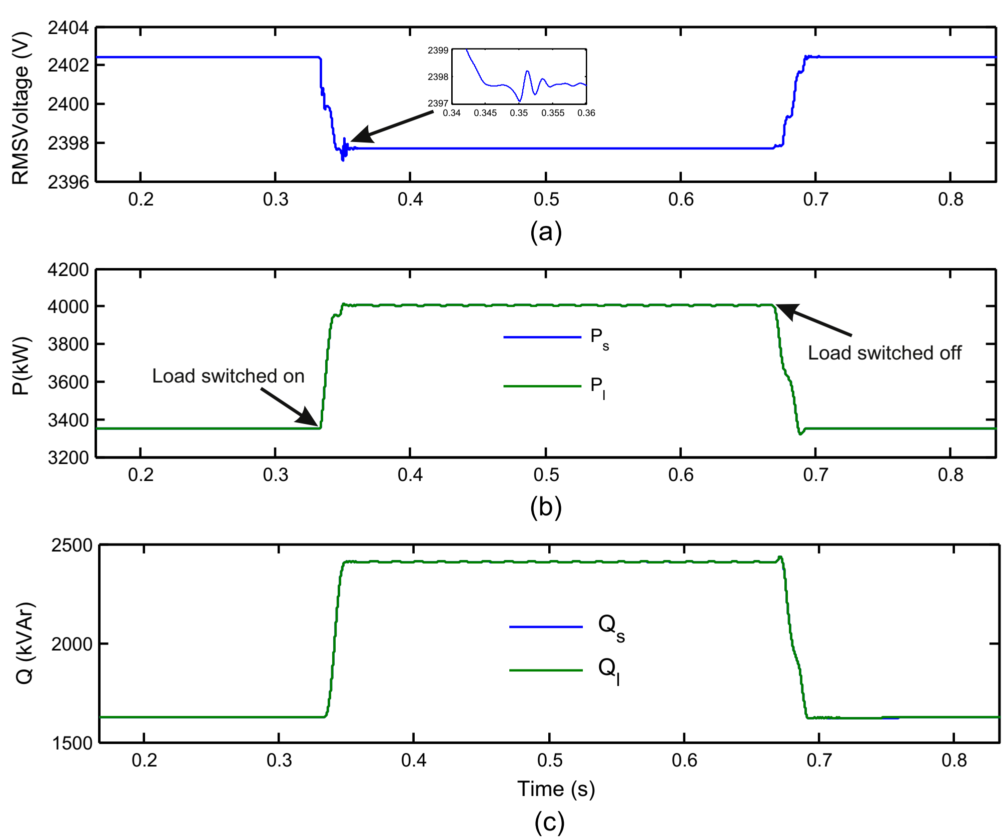

Fig. 6. Load switching without DSTATCOM in the network (a) RMS voltage at bus 632, (b) active power flow and (c) reactive power flow.

Feeder tripping and re-closing

The circuit breaker between the nodes 671 and 692 is opened at 0.33 s to simulate the feeder tripping and re-closed at 0.67 s. The rms value of voltage at bus 632, active and reactive powers flow into the test feeder from utility grid without DSTATCOM in the system are shown in Fig. 4. Tripping of this feeder reduces 1013 kW of active power, 613 kVAr of inductive reactive power and 600 kVAr of capacitive reactive power. It can be observed that total active and reactive powers consumed by the loads in the distribution network are supplied by the utility grid which is verified by overlapping of curves of P_s over P_l in Fig. 4(b) and Q_s over Q_l in Fig. 4(c). Transients in the voltage at the instants of feeder tripping and re-closing are observed having the peak magnitude of 50 V and 20 V respectively. The voltage in this duration has increased by 5 V (approximately). The significant transients in the active and reactive powers have been observed during feeder re-closing as shown in Fig. 4(b) and (c) respectively.

Fig. 5 illustrates the transients associated with feeder tripping and re-closing in the presence of DSTATCOM. The DSTATCOM absorbs active and reactive powers during this period. The power supplied by the utility grid is more compared to the power consumed by the load. Thus, the surplus power is used for battery storage and capacitor charging. Hence, the voltage during this period remains the same. However, transients are observed in the rms value of voltage at the instants of tripping and re-closing of the feeder. The peak magnitude of transient voltages at the time of feeder tripping and re-closing are observed as 10 V and 7 V respectively. Thus, a reduction of 80% at the time of feeder tripping and 65% at the time of feeder re-closing in the peak values of transients have been observed in the presence of DSTATCOM. The transients in the active and reactive powers during feeder re-closing have reduced significantly by the use of DSTATCOM as shown in Fig. 5(b) and (c) respectively. These transients slightly decrease the active power supplied by the DSTATCOM for short duration after feeder re-closing as observed in Fig. 5(b).

The fast Fourier transform (FFT) analysis of voltage signal at bus 632 is carried out. The total harmonic distortion of voltage (THDv) in the absence of DSTATCOM is observed as 0.087%, whereas the same is observed as 0.031% in the presence of DSTATCOM. Thus, 65% reduction in THDv has been achieved by the application of the DSTATCOM.

Load switching

A load comprising of 500 kW active and 500 kVAr reactive powers is switched on at bus 680 by connecting the circuit breaker at 0.33 s and switched off at 0.67 s. The rms value of voltage at bus 632, active and reactive powers flow in the test feeder from utility grid for load switching without DSTATCOM are shown in Fig. 6. It can be observed that additional active and reactive powers demanded by the load are supplied from the utility grid which is verified by overlapping of curves of P_s over P_l in Fig. 6(b) and Q_s over Q_l in Fig. 6(c). Voltage sag is observed due to decrease in voltage magnitude from the value of 2402 V to 2397 V (0.208% voltage sag of magnitude 5 V) at the time of switching on the load and restored to original value after the load is switched off. Transients of low magnitude are observed in the voltage at the time of load switching as shown in Fig. 6(a).

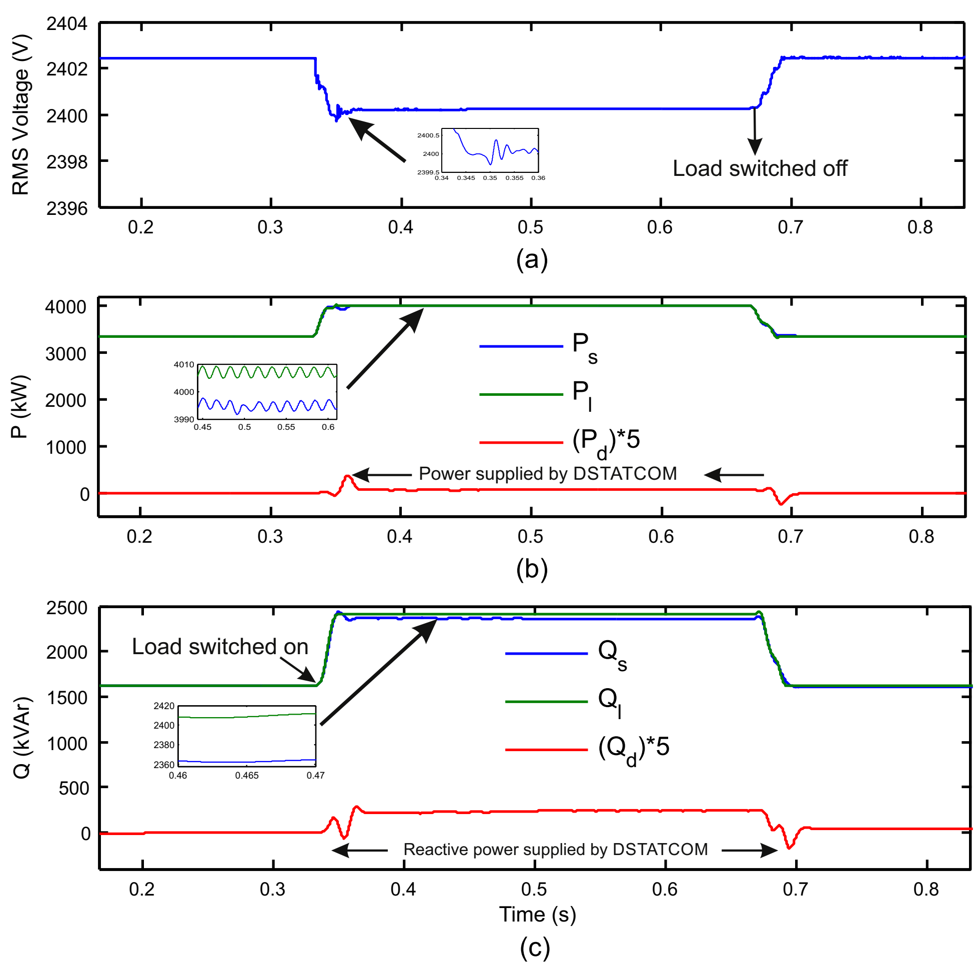

Fig. 7. Load switching with DSTATCOM in the network (a) RMS voltage at bus 632, (b) active power flow and (c) reactive power flow.

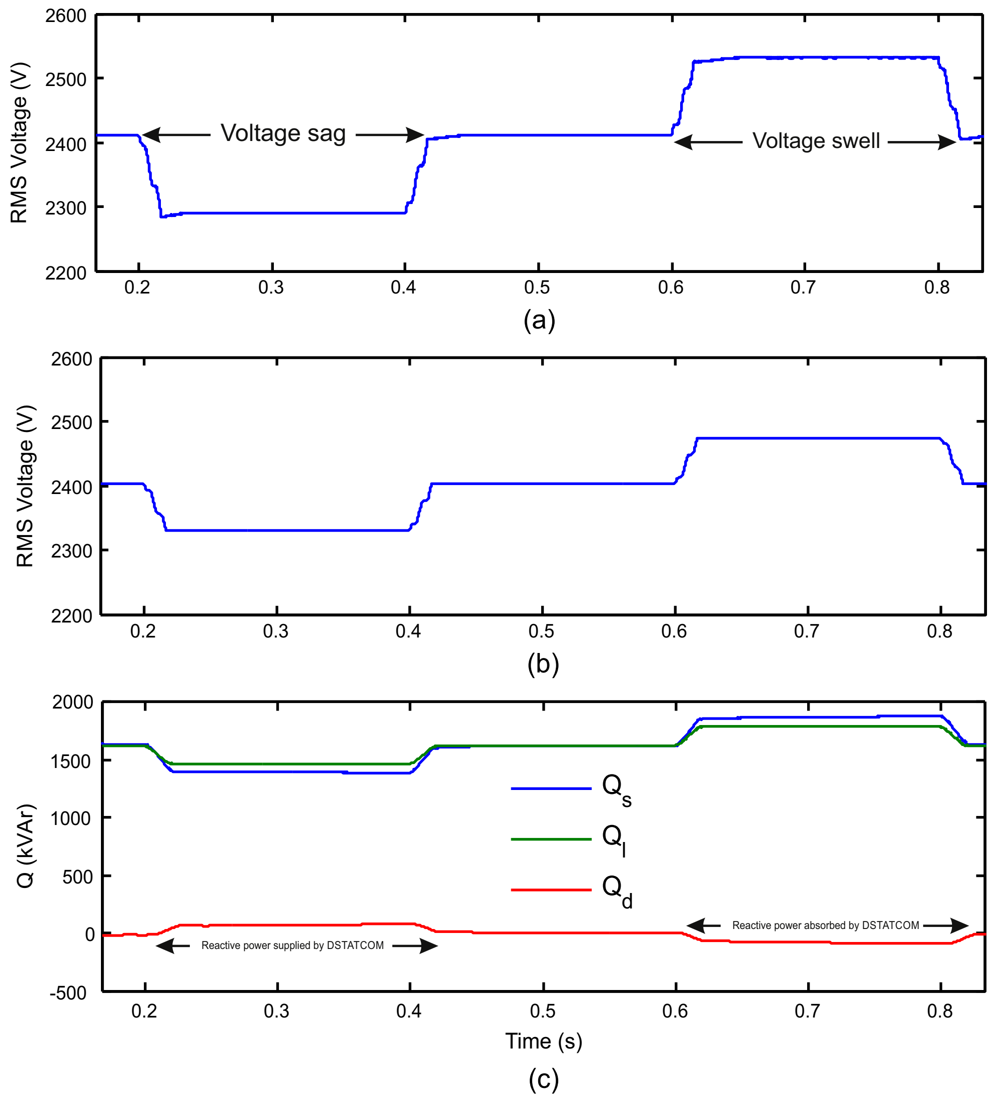

Fig. 8. Voltage sag and swell (a) without DSTATCOM, (b) with DSTATCOM and (c) reactive power flow during voltage sag and swell.

Fig. 7 depicts the rms value of voltage at bus 632, active and reactive powers flow into the test feeder from utility grid for load switching with DSTATCOM. It can be observed that DSTATCOM compensated the active and reactive powers during this period. From Fig. 7(a), it can be observed that voltage sags to 2400 V (0.08325% voltage sag with magnitude of 2 V) in the presence of DSTATCOM. Magnitude of voltage sag is decreased as compared to the case of without DSTATCOM. Hence, a reduction of 60% in the voltage sag has been achieved by the application of DSTATCOM during load switching. The magnitude of voltage transients have also decreased with the compensation provided by DSTATCOM.

The THDv of voltage measured at bus 632 during load switching without DSTATCOM is observed as 0.042%, whereas the same is observed as 0.020% in the presence of DSTATCOM. Thus, 52.38% reduction in THDv has been achieved.

Voltage sag and swell

The voltage sag is simulated by reducing the magnitude of utility grid voltage from 2402 V to 2282 V (5% voltage sag) at 0.2 s and again restoring at 0.4 s. The voltage swell is simulated by increasing the voltage magnitude to 2522 V (5% voltage swell) at 0.6 s and restoring the voltage at 0.8 s. The simulated voltage sag and swell are shown in Fig. 8(a). Voltage sag and swell with DSTATCOM and reactive powers flow are shown in Fig. 8(b) and (c) respectively. It can be observed that in the presence of DSTATCOM, 2.5% of voltage sag is recovered. Similarly, DSTATCOM reduces the swell by 2.5%. Thus, a reduction of 50% in the magnitude of voltage sag and swell has been observed in the presence of DSTATCOM. This improvement in the voltage sag and swell has been observed due to the reactive power exchange between the DSTATCOM and utility grid as shown in Fig. 8(c). Transients in the voltage, active and reactive powers have not been observed during the voltage sags and swells.

THDv of voltage at bus 632 in the absence of DSTATCOM is observed as 0.027%, whereas the same is observed as 0.011% in the presence of DSTATCOM. Thus, 59.26% reduction in THDv has

Table 4
THD of voltage with grid disturbances.

Case studies	THD_v (%)		Improvement in THD_v (%)
	Without DSTATCOM	With DSTATCOM	
Feeder tripping and re-closing	0.087	0.031	65.00
Load switching	0.042	0.020	52.38
Voltage sag and swell	0.027	0.011	59.26

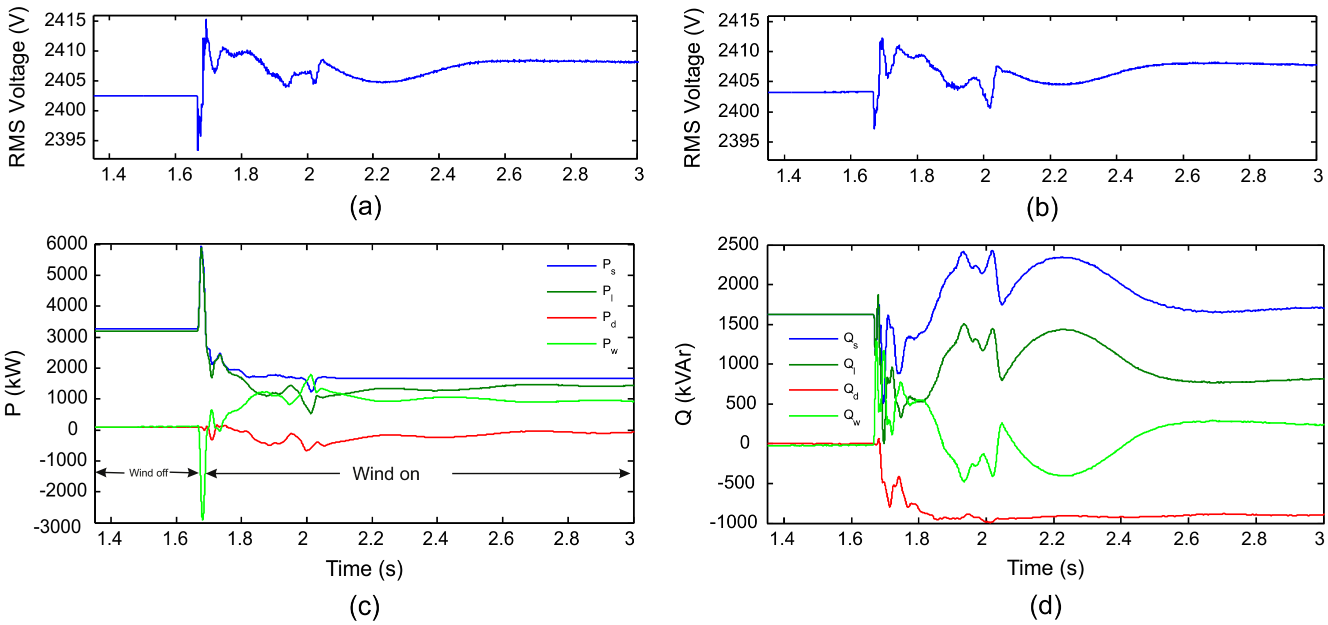

Fig. 9. Wind synchronization (a) voltage without DSTATCOM, (b) voltage with DSTATCOM, (c) active power flow with DSTATCOM and (d) reactive power flow with DSTATCOM.

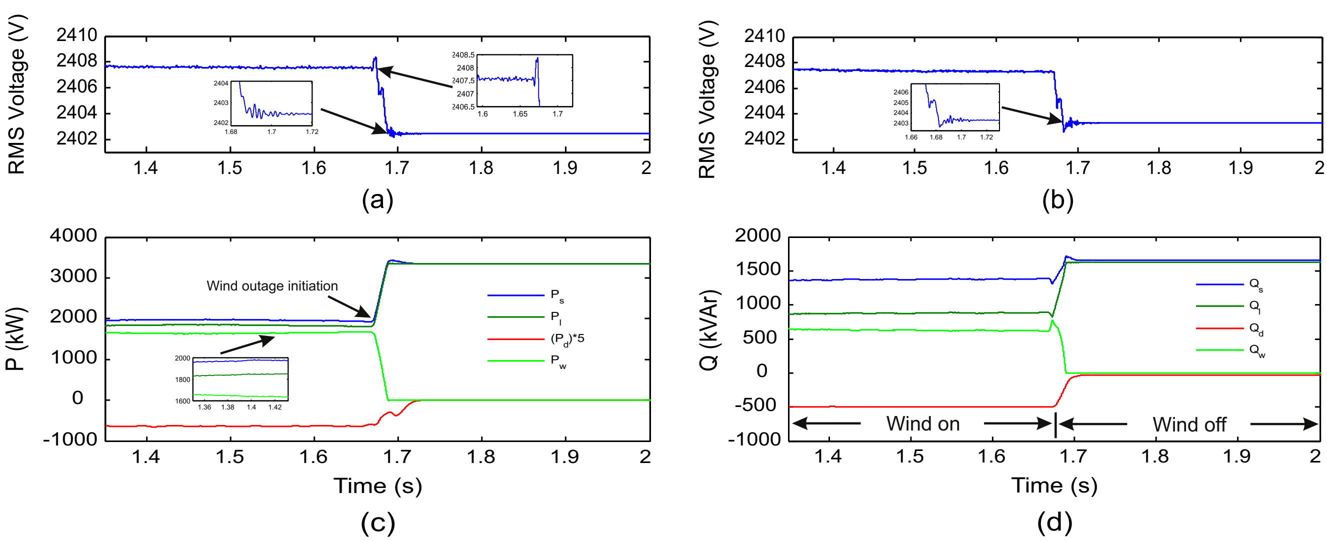

Fig. 10. Wind outage (a) voltage without DSTATCOM, (b) voltage with DSTATCOM, (c) active power flow with DSTATCOM and (d) reactive power flow with DSTATCOM.

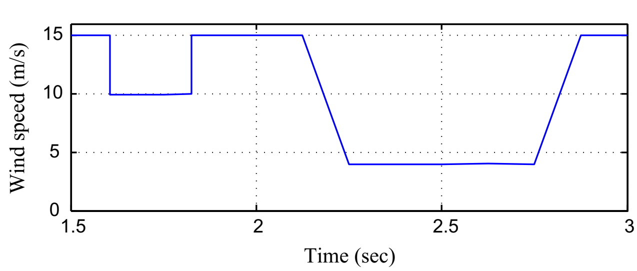

Fig. 11. Wind speed variation.

been achieved by the application of DSTATCOM in the test feeder. The comparative study of THDv in the events of grid disturbances under investigation has been tabulated in Table 4.

Wind energy penetration

The power quality investigations have been made in the events of wind operations such as outage of wind generator, grid synchronization of wind generator and wind speed variations with DSTATCOM in the power network. The active power, reactive power and harmonic compensations have been analyzed in all these events.

Wind synchronization

The circuit breaker used to integrate wind generator is switched on at 1.67 s to simulate the grid synchronization of wind generator. Fig. 9(a) and (b) represent the voltages at bus 632 with and without DSTATCOM. The active and reactive powers flow with DSTATCOM are shown in Fig. 9(c) and (d) respectively. It can be observed that the voltage due to wind penetration has increased from 2402.5 V to 2409 V without DSTATCOM (0.27% increase). This is caused due to

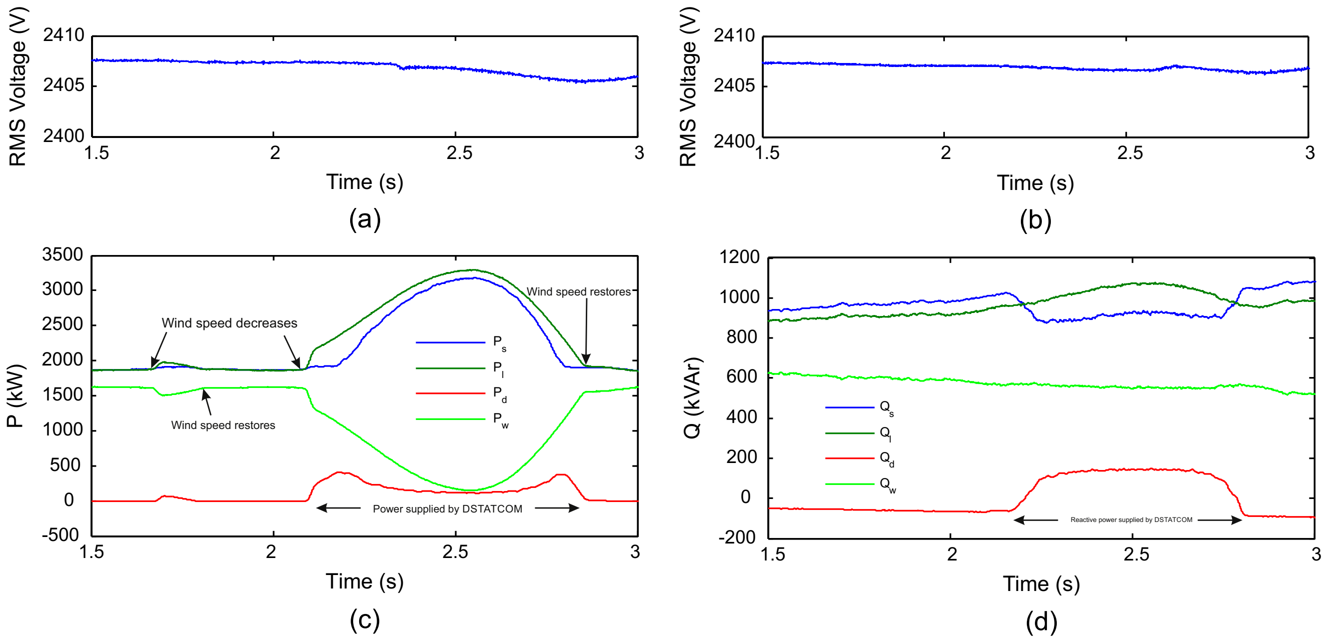

Fig. 12. Wind speed variations (a) voltage without DSTATCOM, (b) voltage with DSTATCOM, (c) active power flow with DSTATCOM and (d) reactive power flow with DSTATCOM.

Table 5
THD of voltage with wind energy penetration.

Case studies	THD_v (%) at bus 632 Without DSTATCOM	With DSTATCOM	Improvement in THD_v (%)
Outage of wind generator	0.84	0.44	47.62
Grid synchronization of wind generator	0.07	0	100
Wind speed variation	0.83	0.42	48.19

available capacitive reactive power compensation with DFIG. In the presence of DSTATCOM wind penetration has increased the voltage to 2407 V (0.18% increase). Hence, improvement in voltage profile has been achieved by the use of DSTATCOM. The peak magnitude of voltage during synchronization has been observed as 12 V and 9 V with and without DSTATCOM as shown in Fig. 9(a) and (b) respectively. Hence, DSTATCOM reduces the peak value of transient voltages through 25%. Thus, an overall improvement in the transient and steady state voltages of bus 632 has been observed with the use of DSTATCOM. The active and reactive powers injected into the network under investigation are reduced due to available local generation of wind. Hence, the surplus active and reactive powers are absorbed by the DSTATCOM during this period. Power transients are observed for a duration of 0.4 s with active power and 0.8 s with reactive power as depicted in Fig. 9(c) and (d) respectively. However, short duration transient of high magnitude available with active power is observed due to inrush current drawn by the DFIG of wind energy conversion system (WECS).

FFT analysis of voltage signal at bus 632 is carried out. THDv of bus voltage in the absence of DSTATCOM is observed as 0.07%. In the presence of DSTATCOM the value of THDv almost reduces to zero. Hence, no harmonic distortion is observed with DSTATCOM in the network.

Wind outage

Wind outage is simulated by opening the circuit breaker connecting the wind generator on bus 680 at 1.67 s. The rms value

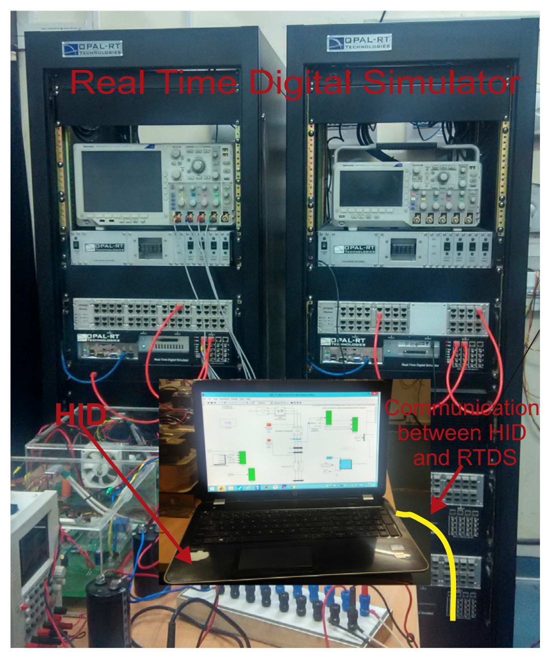

Fig. 13. Experimental set up for real time results.

of voltages at bus 632 with and without DSTATCOM are shown in Fig. 10(a) and (b) respectively. The active and reactive powers flow with DSTATCOM are shown in Fig. 10(c) and (d) respectively. It can be observed that the voltage due to wind outage reduces from 2407.5 V to 2402.5 V without DSTATCOM (reduction by 5 V). In the presence of DSTATCOM wind outage has decreased the bus voltage to 2404 V (reduction by 2.5 V) as shown in Fig. 10(a) and (b) respectively. Thus, improvement in the voltage profile by 50% has been observed by the use of DSTATCOM. The transients in voltage during wind outage have also been reduced significantly by the use of DSTATCOM. Hence, the transient with

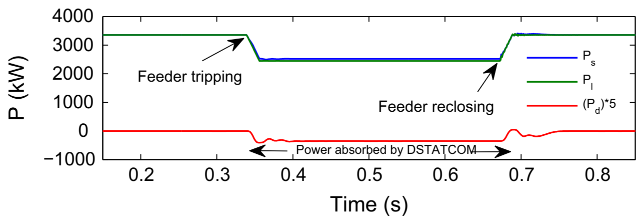

Fig. 14. Real time results of active power flow with feeder tripping and re-closing in the presence of DSTATCOM.

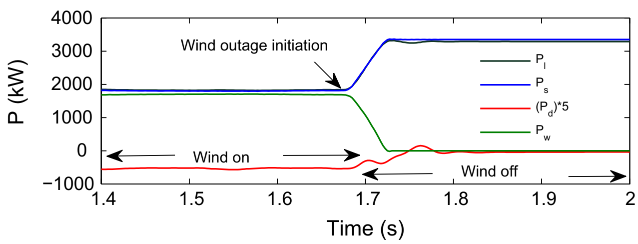

Fig. 15. Real time results of active power flow with wind generator outage in the presence of DSTATCOM.

peak value of 1 V observed without DSTATCOM as sown in Fig. 10 (a) at the moment of switching out the wind generator has not been observed in the presence of DSTATCOM as described in Fig. 10(b). From Fig. 10(c) and (d), it can be observed that the surplus active and reactive powers available with wind generation are used to store energy in the BESS and charging the capacitor. However, the power supplied by the wind and power taken by the DSTATCOM reduces to zero at the moment of wind outage. Low frequency transients are observed in the real power during wind outage. Reactive power is absorbed by the DSTATCOM when the wind generation is available due to the capacitive compensation of DFIG for supplying the reactive power.

The FFT analysis of voltage signal at bus 632 is carried out. The THDv without the use of DSTATCOM is observed as 0.84%, whereas in the presence of DSTATCOM, the THDv reduces to 0.44%. Thus, a reduction of 47.62% in the THDv has been achieved.

Wind speed variation

The variations of wind speed are simulated as shown in Fig. 11, where two changes of low magnitude and high magnitude are investigated. The wind speed abruptly decreases to 10 m/s at 1.6 s and restores at 1.8 s. In the second change, the wind speed decreases to 4 m/s between 2.15 s and 2.7 s.

Fig. 12(a) and (b), represent the voltages at bus 632 with and without DSTATCOM respectively. The active and reactive powers flow with DSTATCOM are shown in Fig. 12(c) and (d) respectively. It can be observed that transients are not observed in the voltage during wind speed variations. However, the magnitude of voltage decreases by 2 V with second change in the wind speed and same is compensated by 50% in the presence of DSTATCOM. From Fig. 12 (c), it can be depicted that slight power variations are observed for the small change in the wind speed and variations of high magnitude are observed with high speed wind gusts. Hence, the power demanded by load is supplied by utility grid and DSTATCOM during this period. The reactive power is not affected by the small wind speed variations. However, the large changes in the wind speed affect the reactive power flow. The reactive power demanded by the load with low wind speed intervals is supplied by the utility grid and DSTATCOM. Hence, it can be observed that DSTATCOM effectively compensates the active and reactive power variations due to changes in the wind speed.

Table 6
Comparison of simulation and real time results in terms of THDv.

Case studies	THD_v (%)		Percentage error (%)
	With DSTATCOM (Simulation)	With DSTATCOM (Real time)	
Feeder tripping and re-closing	0.031	0.03085249	0.047
Load switching	0.020	0.02000710	−0.355
Voltage sag and swell	0.011	0.01050092	0.454
Outage of wind generator	0.44	0.43000185	2.272
Grid synchronization of wind generator	0.00	0.00000000	0.000
Wind speed variation	0.42	0.42804052	−1.914

The THDv of bus voltage in the absence of DSTATCOM is observed as 0.83%, whereas the same reduces to 0.42% by the application of DSTATCOM. Thus, a reduction of 48.19% in the value of THDv has been achieved by the use of DSTATCOM. The comparative study of THDv with wind energy penetration is provided in Table 5. It can be observed that DSTATCOM is highly effective in reduction of harmonics due to wind energy penetration into the distribution network.

Real time validation of results

The validation of simulation results has been carried out on the real time digital simulator of OPAL-RT. The human interface device (HID) interacts with the RTDS. In this study, host laptop with 64-bit operating system, 4 GB RAM, Intel(I) Core(TM) i5-3230 M CPU@2.60 GHz processor is used as HID. The complete set up is shown in Fig. 13. Test system is modelled in MATLAB/Simulink 2011b environment on HID and loaded on ML605 target of RTDS and simulated in hardware synchronization mode to obtain the real time results as good as experimental results. The communication between host laptop and RTDS system is carried out with the help of ether-net communication system. The data are taken out with the help of OpWrite block of the RT-Lab and plotted with the help of MATLAB plot window.

The real time results of active power flow with feeder tripping and re-closing in the presence of DSTATCOM are illustrated in Fig. 14. The real time results of active power flow with outage of wind generator in the presence of DSTATCOM are shown in Fig. 15. These results are very close to their respective simulation results.

The THDv of bus voltage in the presence of DSTATCOM using RTDS are obtained for all cases under study and provided in Table 6. The comparison of real time results with the simulation results has been carried out and an error between these results is obtained. The percentage error (E) in the simulation results compared with the real time results is given by the following relation.

$$E = \left(\frac{SR - RT}{SR}\right) * 100\% \qquad (18)$$

where SR represent the simulation result whereas the RT indicates the real time result. It can be observed from Table 6 that real time results are very close to the simulation results. The percentage error in the value of THDv is below 1% for grid disturbances whereas this error is below 3% for the wind generator operations and wind speed variations. Therefore, the SRF theory based control of DSTATCOM has been proved to be effective for PQ improvement at grid level during the conditions of grid disturbances as well as in the presence of wind power generation.

Conclusion

The proposed research work investigates into PQ events associated with distribution network due to grid disturbances such as voltage sag, swell, load switching, feeder tripping and re-closing. The DSTATCOM has been proposed to improve the power quality in the above events. The proposed DSTATCOM with SRF based control has been proved to be effective in improving the power quality in these events at grid level. The power quality events associated with wind operations such as wind generator outage, grid synchronization of wind generator and wind speed variations have been improved by the use of proposed DSTATCOM in the distribution network. From, these studies it has been established that the DSTATCOM can effectively be used to improve the power quality in the distribution network with wind generation and during grid disturbances. The results have been validated in real time utilizing RTDS. The real time results are very close to the simulation results which shows the effectiveness of proposed DSTATCOM with BESS for improvement of PQ in the distribution system.

References

[1] Ibrahim W, Morcos M. A power quality perspective to system operational diagnosis using fuzzy logic and adaptive techniques. IEEE Trans Power Deliv 2003;18(3):903–9. http://dx.doi.org/10.1109/TPWRD.2003.813885.
[2] Ray P, Mohanty S, Kishor N. Classification of power quality disturbances due to environmental characteristics in distributed generation system. IEEE Trans Sust Energy 2013;4(2):302–13. http://dx.doi.org/10.1109/TSTE.2012.2224678.
[3] Tascikaraoglu A, Uzunoglu M, Vural B, Erdinc O. Power quality assessment of wind turbines and comparison with conventional legal regulations: a case study in turkey. Appl Energy 2011;88(5):1864–72. http://dx.doi.org/10.1016/j.apenergy.2010.12.001.
[4] Dash P, Padhee M, Barik S. Estimation of power quality indices in distributed generation systems during power islanding conditions. Int J Electr Power Energy Syst 2012;36(1):18–30. http://dx.doi.org/10.1016/j.ijepes.2011.10.019.
[5] Mahela OP, Shaik AG, Gupta N. A critical review of detection and classification of power quality events. Renew Sust Energy Rev 2015;41(0):495–505. http://dx.doi.org/10.1016/j.rser.2014.08.070.
[6] Jayaprakash P, Singh B, Kothari D. Three-phase 4-wire dstatcom based on h-bridge vsc with a star/hexagon transformer for power quality improvement. In: IEEE region 10 and the third international conference on industrial and information systems, 2008. ICIIS 2008; 2008. p. 1–6. http://dx.doi.org/10.1109/ICIINFS.2008.4798378.
[7] Mahela OP, Shaik AG. Topological aspects of power quality improvement techniques: a comprehensive overview. Renew Sust Energy Rev 2016;58:1129–42. http://dx.doi.org/10.1016/j.rser.2015.12.251.
[8] Shukla A, Ghosh A, Joshi A. Control schemes for dc capacitor voltages equalization in diode-clamped multilevel inverter-based DSTATCOM. IEEE Trans Power Deliv 2008;23(2):1139–49. http://dx.doi.org/10.1109/TPWRD.2008.915804.
[9] Arya S, Singh B, Chandra A, Al-Haddad K. Learning-based anti-hebbian algorithm for control of distribution static compensator. IEEE Trans Ind Electron 2014;61(11):6004–12. http://dx.doi.org/10.1109/TIE.2014.2321341.
[10] Sahu G, Mahapatra K. A novel control strategy of dstatcom for load compensation under distorted utility condition. In: 2014 international conference on advances in electrical engineering (ICAEE); 2014. p. 1–6. http://dx.doi.org/10.1109/ICAEE.2014.6838502.
[11] Singh B, Niwas R. Power quality improvements in diesel engine driven induction generator system using srf theory. In: 2012 IEEE fifth power India conference; 2012. p. 1–5. http://dx.doi.org/10.1109/PowerI.2012.6479569.
[12] Mahela OP, Shaik AG. A review of distribution static compensator. Renew Sust Energy Rev 2015;50:531–46. http://dx.doi.org/10.1016/j.rser.2015.05.018.
[13] Ghosh A, Joshi A. The concept and operating principles of a mini custom power park. IEEE Trans Power Deliv 2004;19(4):1766–74. http://dx.doi.org/10.1109/TPWRD.2003.822541.
[14] Virulkar V, Aware M. Dstatcom with bess, an efficient means for flicker mitigation. In: TENCON 2008 – 2008 IEEE region 10 conference; 2008. p. 1–6. http://dx.doi.org/10.1109/TENCON.2008.4766740.
[15] Bhattacharjee C, Roy A, Roy B. Improvement of available load voltage for a constant speed wecs coupled with fuzzy-controlled dstatcom. In: 2012 IEEE 15th international conference on harmonics and quality of power (ICHQP); 2012. p. 637–41. http://dx.doi.org/10.1109/ICHQP.2012.6381304.
[16] Singh A, Bhowmick S, Shukla K. Load compensation with dstatcom and bess. In: 2012 IEEE 5th India international conference on power electronics (IICPE); 2012. p. 1–6. http://dx.doi.org/10.1109/IICPE.2012.6450494.
[17] Woo S-M, Kang D-W, Lee W-C, Hyun D. Seok. The distribution statcom for reducing the effect of voltage sag and swell. In: The 27th annual conference of the IEEE industrial electronics society, 2001, IECON '01, vol. 2; 2001. p. 1132–7. http://dx.doi.org/10.1109/IECON.2001.975939.
[18] Yuvaraj V, Deepa S, Rozario A, Kumar M. Improving grid power quality with facts device on integration of wind energy system. In: 2011 fifth Asia modelling symposium (AMS); 2011. p. 157–62. http://dx.doi.org/10.1109/AMS.2011.38.
[19] Kersting W. Radial distribution test feeders. IEEE Trans Power Syst 1991;6(3):975–85. http://dx.doi.org/10.1109/59.119237.
[20] Paz MCR, Ferraz RG, Bretas AS, Leborgne RC. System unbalance and fault impedance effect on faulted distribution networks. Comput Math Appl 2010;60(4):1105–14. http://dx.doi.org/10.1016/j.camwa.2010.03.067. pCO 2010 gold coast, Australia 24th December 2010 3rd global conference on power control optimization.
[21] Mahela OP, Shaik AG. Power quality detection in distribution system with wind energy penetration using discrete wavelet transform. In: IEEE international conference on advances in computing and communication engineering (ICACCE), 2015 IEEE; 2015. pp. 1–6.
[22] Mahela OP, Shaik AG. Comprehensive overview of grid interfaced wind energy generation systems. Renew Sust Energy Rev 2016;57:260–81. http://dx.doi.org/10.1016/j.rser.2015.12.048.
[23] Mitra P, Venayagamoorthy G. An adaptive control strategy for DSTATCOM applications in an electric ship power system. IEEE Trans Power Electron 2010;25(1):95–104. http://dx.doi.org/10.1109/TPEL.2009.2024152.
[24] Kumar C, Mishra M. A modified DSTATCOM topology with reduced VSI rating, DC link voltage, and filter size. In: 2013 international conference on clean electrical power (ICCEP); 2013. p. 325–31. http://dx.doi.org/10.1109/ICCEP.2013.6587009.
[25] Singh B, Jayaprakash P, Kothari D, Chandra A, Al Haddad K. Comprehensive study of DSTATCOM configurations. IEEE Trans Ind Inform 2014;10(2):854–70. http://dx.doi.org/10.1109/TII.2014.2308437.
[26] Rohilla Y, Pal Y. T-connected transformer integrated three-leg VSC based 3P4W DSTATCOM for power quality improvement. In: 2013 Nirma University international conference on engineering (NUiCONE); 2013. p. 1–7. http://dx.doi.org/10.1109/NUiCONE.2013.6780146.
[27] Labeeb M, Lathika B. Design and analysis of DSTATCOM using SRFT and ANN-fuzzy based control for power quality improvement. In: Recent advances in intelligent computational systems (RAICS), 2011 IEEE; 2011. p. 274–79. http://dx.doi.org/10.1109/RAICS.2011.6069317.
[28] Singh B, Arya S, Jain C, Goel S. Implementation of four-leg distribution static compensator. Gener Transm Distrib, IET 2014;8(6):1127–39. http://dx.doi.org/10.1049/iet-gtd.2013.0582.
[29] Singh B, Jayaprakash P, Kothari D. A T-connected transformer and three-leg VSC based DSTATCOM for power quality improvement. IEEE Trans Power Electron 2008;23(6):2710–8. http://dx.doi.org/10.1109/TPEL.2008.2004273.
[30] Singh B, Jayaprakash P, Kothari D. Isolated h-bridge VSC based 3-phase 4-wire DSTATCOM for power quality improvement. In: IEEE international conference on sustainable energy technologies, 2008. ICSET 2008; 2008. p. 366–71. http://dx.doi.org/10.1109/ICSET.2008.4747034.
[31] Singh B, Jayaprakash P, Somayajulu T, Kothari D. Reduced rating VSC with a zig-zag transformer for current compensation in a three-phase four-wire distribution system. IEEE Trans Power Deliv 2009;24(1):249–59. http://dx.doi.org/10.1109/TPWRD.2008.2005398.
[32] Singh B, Sharma S. Design and implementation of four-leg voltage-source-converter-based VFC for autonomous wind energy conversion system. IEEE Trans Ind Electron 2012;59(12):4694–703. http://dx.doi.org/10.1109/TIE.2011.2179271.
[33] Singh B, Niwas R, Kumar Dube S. Load leveling and voltage control of permanent magnet synchronous generator-based DG set for standalone supply system. IEEE Trans Ind Inform 2014;10(4):2034–43. http://dx.doi.org/10.1109/TII.2014.2341952.
[34] Zaveri T, Bhavesh B, Zaveri N. Control techniques for power quality improvement in delta connected load using dstatcom. In: 2011 IEEE international electric machines drives conference (IEMDC); 2011. p. 1397–402. http://dx.doi.org/10.1109/IEMDC.2011.5994811.
[35] Singh B, Solanki J. A comparison of control algorithms for DSTATCOM. IEEE Trans Ind Electron 2009;56(7):2738–45. http://dx.doi.org/10.1109/TIE.2009.2021596.